

EN-TensorCore: Advancing TensorCores Performance through Encoder-Based Methodology

Qizhe Wu

University of Science and Technology
of China
Hefei, China
wqz1998@mail.ustc.edu.cn

Yuchen Gui

University of Science and Technology
of China
Hefei, China
guiyuchen@mail.ustc.edu.cn

Zhichen Zeng

University of Science and Technology
of China
Hefei, China
zhichenzeng@mail.ustc.edu.cn

Xiaotian Wang

University of Science and Technology
of China
Hefei, China
wxtsdg@mail.ustc.edu.cn

Huawen Liang

University of Science and Technology
of China
Hefei, China
lhw233@mail.ustc.edu.cn

Xi Jin

University of Science and Technology
of China
Hefei, China
jinxi@ustc.edu.cn

ABSTRACT

Tensor computations, with matrix multiplication being the primary operation, serve as the fundamental basis for data analysis, physics, machine learning, and deep learning. As the scale and complexity of data continue to grow rapidly, the demand for tensor computations has also increased significantly. To meet this demand, several research institutions have started developing dedicated hardware for tensor computations. To further improve the computational performance of tensor process units, we have reexamined the issue of computation reuse that was previously overlooked in existing architectures. As a result, we propose a novel EN-TensorCore architecture that can significantly reduce chip area and power consumption. Furthermore, our method is compatible with existing tensor processing architectures. We evaluated our method on prevalent microarchitectures, the results demonstrate an average improvement in area efficiency of 8.7%, 12.2%, and 11.0% for tensor computing units at computational scales of 256 GOPS, 1 TOPS, and 4 TOPS, respectively. Similarly, there were energy efficiency enhancements of 13.0%, 17.5%, and 15.5%.

KEYWORDS

Tensor Process Unit; Hardware Acceleration; Multiplier; AI accelerator; Tensor Cores; Neural Process Unit

1 INTRODUCTION

Tensors, essentially multi-dimensional matrix extensions, offer an efficient way to represent complex data including images, sound, and text, and are fundamental to various analytical tasks in data analysis, physics, and machine learning, especially deep learning algorithms, with matrix multiplication being a key operation.

The surge in data and intricacy has significantly boosted the need for tensor-based computations, as AI has evolved from a marginal area research topic to a core driver of modern technology over the last decade. AI applications, including search engines, generative AI based on Large Language Models (LLMs), and tools for self-driving cars, have become widespread in everyday life. Many of these AI applications rely on large-scale tensor computations, leading to specialized hardware development for these calculations by researchers. Include NVIDIA's incorporation of Tensor Cores[1]

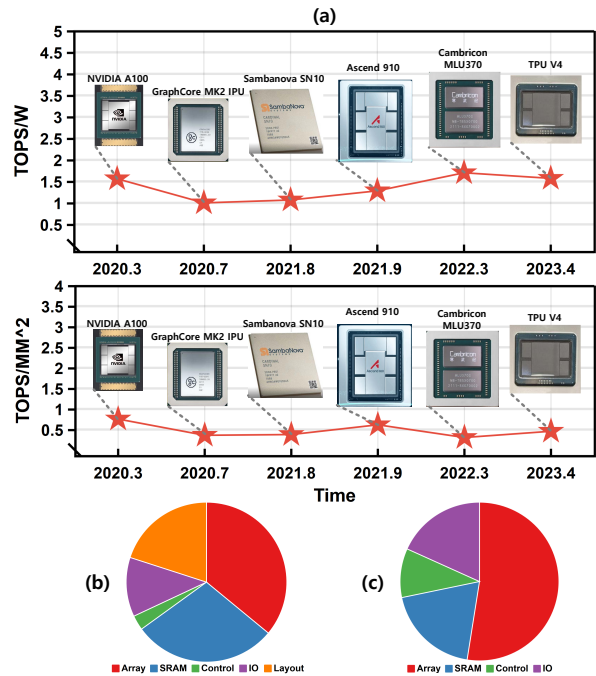


Figure 1: Performance Analysis of AI Accelerators

in their Volta, Turing, Ampere, and the latest Hopper architectures; Google's Tensor Processing Unit (TPU)[2]; Graphcore's MK series Intelligence Processing Unit (IPU)[3]; SambaNova's SN[4] series deep learning processors; HUAWEI's Ascend[5]; and Cambricon's Machine Learning Unit (MLU)[6]. For mobile devices, the Snapdragon 8gen3[7], MediaTek Dimensity 9300[8], and Apple A17[9] have all integrated neural processing units to enhance the energy efficiency of generative AI in mobile SoCs.

Fig. 1(a) shows the INT8 on-chip die performance of 7nm AI processors that have been successfully commercialized in recent years. The rate of performance improvement is gradually decelerating and approaching a stable state. Typical microarchitectures include the 2D Matrix (Fig. 2(a)) of Cambricon's DianNao[10] and the 1D/2D Array (Fig. 2(b)) of Cambricon's DaDianNao[11], the Systolic Array (Output Stationary (OS) and Weight Stationary (WS))[12] (Fig.

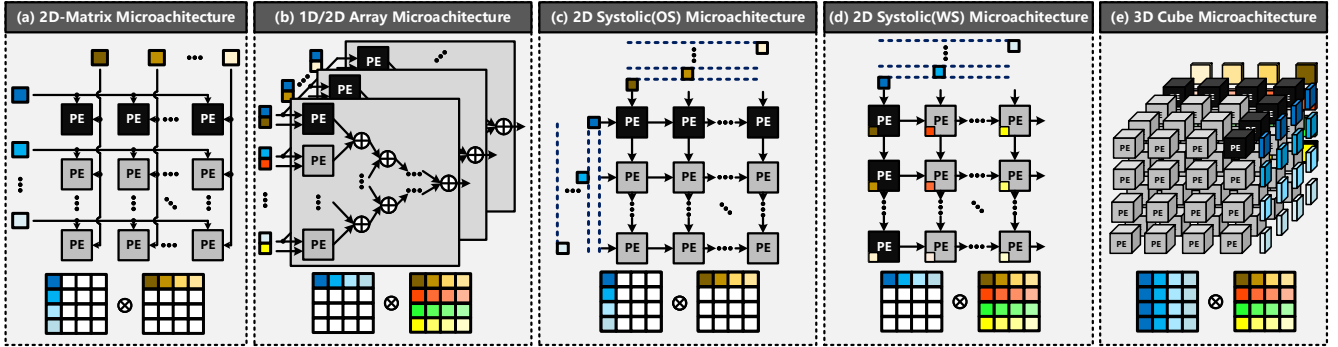


Figure 2: Mainstream Microarchitectures of Tensor Computing Units in Recent Years

2(c-d)) of TPU and the speculative Tesla FSD[13], as well as the 3D Cube (Fig. 2(e)) of Ascend [5] and NVIDIA [14]. The primary distinction among these architectures lies in the optimization and alteration of the data flow paths and interconnect topologies within the multiplier arrays, aiming to enhance data reuse for matrix multiplication within the Tensor Computing Units (TCUs). Although some of these architectures were proposed many years ago, they continue to be widely applied in commercial AI processors and academic AI accelerators. Fig. 1(b)(c) presents the floor plan of the TPU die[2], showing the area (Fig. 1(b)) and power (Fig. 1(c)) consumption distribution. The TCUs, SRAM, and layout wiring occupy 85% of the die area, with the TCUs (including the multiplier arrays, accumulators, and pipeline registers) accounting for the highest proportion of the area. In terms of power consumption, the TCUs are the primary contributors to the on-chip power. Given the critical role of the TCUs in providing computational power for AI accelerators, optimizing the architecture of these units is particularly crucial for further performance enhancements.

Our contribution is as follows: (1) We conducted a comprehensive exploration of potential computation reuse in tensor calculations in existing TCUs. To address this, we propose a novel computational paradigm and architecture called EN-TensorCore, and developed a novel data encoding representation. This approach offers high versatility and can be seamlessly integrated into existing TCUs to minimize chip area and power; (2) We have evaluated our method across prevalent tensor computational microarchitectures in Fig. 2(a~e). Our results demonstrate an average area efficiency improvement of 8.7%, 12.2%, and 11.0% for TCUs at computational scales of 256 GOPS, 1 TOPS, and 4 TOPS, respectively. Similarly, energy efficiency enhancements of 13.0%, 17.5%, and 15.5%.

2 MOTIVATION

The numerous operators within deep neural networks can be represented as multi-level nested loops; for instance, matrix multiplication can be depicted as a triply nested loop (excluding the batch size dimension). By spatially unrolling and temporally reordering these loop dimensions, it is possible to research data reuse within accelerators to enhance both energy efficiency and computational power. Such data reuse can also be interpreted as a single multiplicand being multiplied by multiple multipliers across temporal or spatial dimensions. For example, in a 2D Matrix, all row PEs perform the

same multiplicand by different multipliers in the spatial dimension; in a Systolic Array (OS), all row PEs perform the same multiplicand by different multipliers at different times; similarly, we can observe in other architectures that this behavior exists in all rows or columns of the multiplier array. Essentially, this phenomenon is due to data reuse, so we believe there may still be unexplored repeated computations in large-scale TCUs. This repetition may be caused by the same multiplicand by different multipliers.

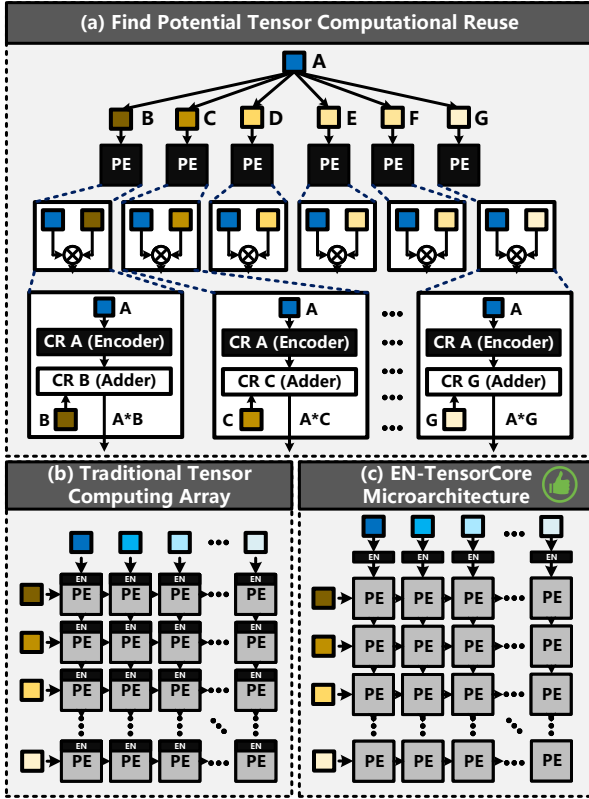
3 METHODOLOGY

3.1 EN-TensorCore Architecture

In the design of multipliers in modern computer systems, the multiplication ($A \times B$) involves three key steps. First, partial products of the multiplier B are generated; second, all the partial products are compressed to produce the final row of sums and carries; lastly, a full adder is used to accumulate the sums and carries to obtain the product result. Many designs adopt the Modified Booth Encoding (MBE)[15–18] for the first step (Fig. 4), as it can reduce the number of partial product rows for an n -bit fixed-point multiplication by half to $n/2$, significantly decreasing the latency and hardware cost. This involves encoding the multiplicand A and using the encoded A and the multiplier B to generate partial products. Next, in the second step, methods such as Wallace Tree[19] or Compressor Tree[20] are used to compress the partial products, effectively reducing the number of partial product rows to the final two rows (sums and carries). In the third step, designers often employ advanced adder technologies, such as carry-lookahead adders or carry-select adders[21], to merge these two rows, thereby yielding the final product result.

Considering a single multiplication operation, we can draw two conclusions: first, the encoding part is a logical computation related only to the multiplicand A and is independent of the multiplier B ; second, the result of the multiplication is directly related to the encoded multiplicand A and the multiplier B , and indirectly related to the origin multiplicand A .

When we extend this behavior to arrays of multipliers, since matrix multiplication or convolution has phenomenon of same multiplicand by different multiplier in the spatial dimension or time dimension, there is a repeated encoding behavior of the multiplicand A inside the multiplier of PEs (Fig. 3(a)). From the perspective of TCUs, what is needed is the encoded multiplicand A , not A itself. When applied to the existing various TCUs hardware architectures,


Figure 3: The Architecture of EN-TensorCore

whether it's based on data broadcasting like 2D Matrix or 1D/2D Array, or data flow-based like Systolic Array or 3D Cube, enhancing performance only requires the following simple steps: First, remove the encoder logic from all multipliers within the tensor cores (Fig. 3(b)), retaining only the partial product compressor and the full adder; second, add a single encoder to each column of the multiplicand pathway outside the array (Fig. 3(c)), allowing the encoded multiplicand A to flow or broadcast within the array. In terms of area, this can reduce the size of an individual PE, and when applied to TCUs with large-scale multiplier arrays, it can make the array layout more efficient and compact, which is beneficial for reducing the latency of multiplication operations. In terms of power consumption, it not only saves the power consumption caused by repetitive encoding logic, but also, due to the reduced array area, makes the data transmission pathways between adjacent PEs shorter, which further reduces the power consumption associated with data flow between PEs.

3.2 Challenge in Modified Booth Encoding

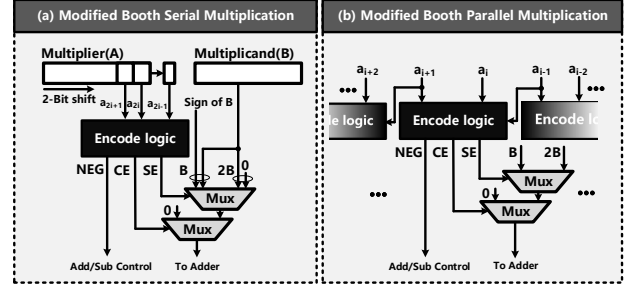
Considering the multiplication of two n -bit integer A (multiplicand) and B (multiplier) in 2's complement representation, i.e.,

$$\begin{aligned} A &= -a_{n-1}2^{n-1} + \sum_{i=0}^{n-2} a_i 2^i \\ B &= -b_{n-1}2^{n-1} + \sum_{i=0}^{n-2} b_i 2^i \end{aligned} \quad (1)$$

in MBE, A is transformed into:

$$A = \sum_{i=0}^{\frac{n}{2}-1} m_i 2^{2i} = \sum_{i=0}^{\frac{n}{2}-1} (-2a_{2i+1} + a_{2i} + a_{2i-1}) 2^{2i} \quad (2)$$

where $a_{-1} = 0$, and $m_i \in \{-2, -1, 0, 1, 2\}$.


Figure 4: Modified Booth Multiplier

Based on the encoding result of A (the logical expression as in Eq. 3), Booth selectors choose $-2B$, $-B$, 0 , B , or $2B$ to generate the partial product rows of $A \times B$ (Fig. 4(a)). For a single-cycle multiplier, $n/2$ encoders are required to encode the multiplicand in parallel (Fig. 4(b)).

$$\begin{aligned} NEG &= \overline{a_{2i+1}} (\overline{a_{2i}} + \overline{a_{2i-1}}) \\ SE &= \overline{a_{2i+1}} a_{2i} a_{2i-1} + a_{2i+1} \overline{a_{2i}} \overline{a_{2i-1}} \\ CE &= a_{2i} \oplus a_{2i-1} + SE \end{aligned} \quad (3)$$

MBE can be viewed as digit-set conversion: the recoding takes a radix-4 number with digits in $[0, 3]$ and converts it to the digit set $[-2, 2]$. The digit-set conversion process defined by radix-4 Booth's recoding entails no carry propagation. Each radix-4 digit in $[-2, 2]$ is obtained, independently from all others, by examining 3 bits of the multiplicand, with consecutive 3-bit segments overlapping in 1 bit. Thus, radix-4 Booth's recoding is said to be based on overlapped 3-bit scanning of the multiplicand.

However, applying MBE to the EN-TensorCore architecture does not achieve the expected effect. This is because every 2 bits of the multiplicand need to be encoded into 3 bits to serve as control lines NEG, SE, CE. Thus, for the multiplication of two n -bit numbers, the multiplicand needs to be encoded into $[n/2] * 3$ bits. Externalizing the encoder would actually cause the width of the interconnects between multiplicands in the TCUs, which is undesirable. The increase in interconnect width significantly affects the chip's area and power. To address this, we redesigned an encoder that encodes an n -bit multiplicand into $n + 1$ bits to reduce the width of the encoded numbers, which will be described in the subsection 3.3.

3.3 Modified Encoding in EN-TensorCore

3.3.1 Construction of Encoding Polynomials. From Eq. 2, it can be found that the intrinsic reason for the high bit width of the MBE is that the encoding coefficients m_i have five different states $\{-2, -1, 0, 1, 2\}$, therefore requiring 3 bits of control lines to select the corresponding multiplier. One approach is to start by compressing the number of states in the coefficients of the powers. We

consider this issue from the perspective of the number decomposition; the partial product of $A \times B$ depends on the number of terms A is decomposed into. A number with n bits (we assume that n is an even integer) can be decomposed into $n/2$ terms by MBE, which means that the composition of each term must include powers of 4. Thus, an n -bit unsigned number can be decomposed into the following polynomial, where a_i is a 2-bit unsigned number, and $a_i \in \{0, 1, 2, 3\}$, $N = \frac{n}{2}$, $Q_N \in [0, 2^n - 1]$.

$$Q_N = \sum_{i=0}^N a_i 4^i \quad (4)$$

$Q_N \in [0, 2^{n-1} + (2^{n-2} - 1)]$ when $a_{N+1} \in \{0, 1, 2\}$, $a_i \in \{0, 1, 2, 3\}$.

We aim to avoid the occurrence of 3 in the coefficients of the polynomial, as we cannot directly obtain the product of 3 and the multiplier B through shift operations. Consequently, we have re-structured the coefficients of the polynomial Q' as Eq. 5, where $Cin_{n+1} \in \{0, 1\}$. For $w_i \in \{0, 1, 2, -1\}$, we encode it in binary format and correspondingly map it to $\{00, 01, 10, 11\}$. We denote the encoding result as $Encode(w)$.

$$Q'_N = Cin_{N+1} 4^{N+1} + \sum_{i=0}^N w_i 4^i \quad (5)$$

If we can express Q in the form of Q' , then we can transform the multiplication operation into several simple shift and addition operations. The current issue is whether we can find such a set of solutions $\{Cin_{N+1}, w_N, w_{N-1}, \dots, w_0\}$ that satisfies $Q' = Q$. We will use mathematical induction to prove the existence of such solutions and obtain their recursive expression.

When $n = 0$, we have the following equation:

$$Q_0 = a_0, \quad Q'_0 = Cin_1 4 + w_0 \quad (6)$$

The equation $Q_0 = Q'_0$ holds true when we let:

$$w_0 = \begin{cases} a_0, & a_0 \in \{0, 1, 2\} \\ -1, & a_0 = 3 \end{cases}, \quad Cin_1 = \begin{cases} 0, & a_0 \in \{0, 1, 2\} \\ 1, & a_0 = 3 \end{cases} \quad (7)$$

At this point, the binary encoding of the signed number w_0 and the 2-bit unsigned number a_0 are identical. This can be further expressed as:

$$Encode(w_0) = [a_0]_2, \quad Cin_1 = a_0 [1] \& a_0 [0] \quad (8)$$

where $[a]_2$ denotes the binary encoding of the number a , and $a [i]$ represents the i th bit of a in its binary encoding.

When $n = 1$, we have:

$$Q_1 = a_1 4 + a_0, \quad Q'_1 = Cin_2 4^2 + w_1 4 + w_0 \quad (9)$$

Substituting Eq. 6 into Eq. 9 results in:

$$\begin{aligned} Q_1 &= (a_1 + Cin_1) 4 + w_0 \\ &= a'_1 4 + w_0 \end{aligned} \quad (10)$$

where $a'_1 = (a_1 + Cin_1) \in \{0, 1, 2, 3, 4\}$.

Letting:

$$w_1 = \begin{cases} a'_1, & a'_1 \in \{0, 1, 2\} \\ a'_1 - 4, & a'_1 \in \{3, 4\} \end{cases}, \quad Cin_2 = \begin{cases} 0, & a'_1 \in \{0, 1, 2\} \\ 1, & a'_1 \in \{3, 4\} \end{cases} \quad (11)$$

Then $Q_1 = Q'_1$, and w_1 and Cin_2 can be expressed as:

$$\begin{aligned} Encode(w_1) &= [a'_1]_2 + Cin_1 \\ Cin_2 &= (a_1 [1] \& a_1 [0]) | (a_1 [1] \& Cin_1) \end{aligned} \quad (12)$$

Assume $Q_m = Q'_m$ holds true, this implies:

$$\sum_{i=0}^m a_i 4^i = Cin_{m+1} 4^{m+1} + \sum_{i=0}^m w_i 4^i \quad (13)$$

To ensure that $Q_{m+1} = Q'_{m+1}$, it is equivalent to proving $Q_{m+1} - Q_m = Q'_{m+1} - Q'_m$, which can be expressed as:

$$(a_{m+1} + Cin_{m+1}) 4^{m+1} = Cin_{m+2} 4^{m+2} + w_{m+1} 4^{m+1} \quad (14)$$

This can be simplified to:

$$a'_{m+1} = Cin_{m+2} 4 + w_{m+1} \quad (15)$$

where $a'_{m+1} = a_{m+1} + Cin_{m+1}$. Similar to the values in Eq. 11 and the encoding method in Eq. 12, we can select the following expression to ensure Eq. 15 holds true:

$$w_{m+1} = \begin{cases} a'_{m+1}, & a'_{m+1} \in \{0, 1, 2\} \\ a'_{m+1} - 4, & a'_{m+1} \in \{3, 4\} \end{cases}, \quad Cin_{m+2} = \begin{cases} 0, & a'_{m+1} \in \{0, 1, 2\} \\ 1, & a'_{m+1} \in \{3, 4\} \end{cases} \quad (16)$$

$$Encode(w_{m+1}) = [a_{m+1}]_2 + Cin_{m+1}$$

$$Cin_{m+2} = (a_{m+1} [1] \& a_{m+1} [0]) | (a_{m+1} [1] \& Cin_{m+1}) \quad (17)$$

Based on the foregoing analysis, we have demonstrated that for $n = 2$ and $n = m$, through the recursive expressions Eq. 16 and Eq. 17, a set of solutions $\{Cin_{N+1}, w_N, w_{N-1}, \dots, w_0\}$ can be identified, enabling the polynomial Q_N to be expressed as the polynomial Q'_N . According to the principle of mathematical induction, for all $N \geq 2$, we can employ a recursive method to represent the polynomial Q_N as the polynomial Q'_N . Hence, based on Eq. 7, 8, 16 and 17, we can encode an n -bit unsigned number into $n/2$ two-bit coefficients and one one-bit coefficient.

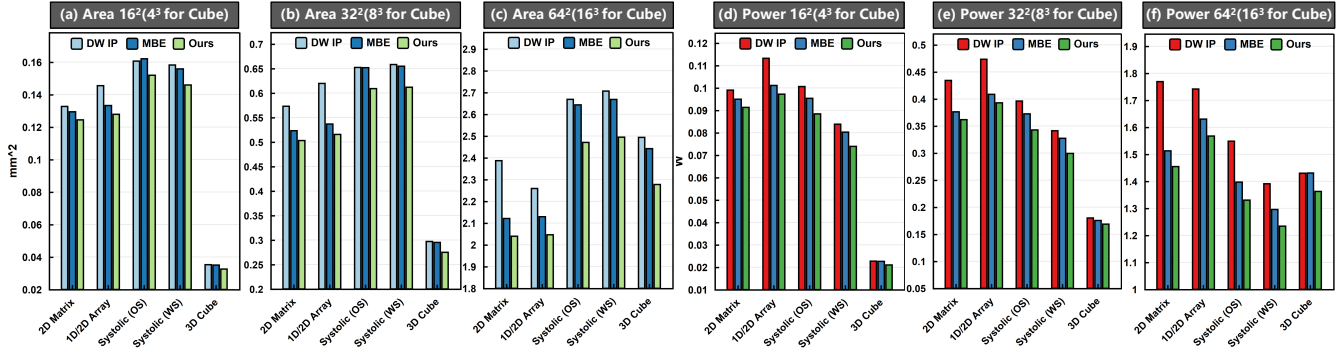
For example, $78(\text{int}8)$ is encoded as $Encode(78) = \{0, 1, 1, -1, 2\}$, therefore the multiplication result of B and 78 is $B4^3 + B4^2 - B4^1 + 2B$. The subsequent calculations are completely identical to those of MBE, that is, B with different bit weights is added together to obtain the final multiplication result. When A is negative, it is only necessary to perform a transformation on B based on the sign bit of A to implement signed multiplication (at this point, the hardware will choose $-B$ as the B in the above formula to participate in the actual calculation).

In terms of the number of encoders, for an n -bit signed number using MBE, $n/2$ encoders are required; we need $(n/2 - 1)$ encoders (as the lowest 2 bits do not need encoding). For the encoded bit width, MBE requires $[n/2] * 3$ bits, whereas our method requires $n + 1$ bits. In the experimental section, we will first perform an evaluation of the area, delay, and other performance metrics of encoders for different bit widths, and test the performance of the optimized encoders within the EN-TensorCore.

4 EXPERIMENT

4.1 Implement Environment

We implement our design in RTL and then synthesize, place and route it with Synopsys Design Compiler toolchain using the SMIC 40nm NLL-HS-RVT technology. We evaluate the performance and


Figure 5: Experiments of Area and Power of EN-TensorCore

Single Encoder Comparison					
Method	AND	NAND	NOR	XNOR	Area
MBE	2	2	1	1	7.06
Ours	1	3	0	2	8.64

Comparison of High Bit Encoders						
Width	Method	Area	Delay	Power	Number	En-Width
8	MBE	28.22	0.23	24.06	4	12
	Ours	25.93	0.36	21.47	3	9
10	MBE	35.28	0.23	30.07	5	15
	Ours	34.57	0.45	28.47	4	11
12	MBE	42.34	0.23	36.03	6	18
	Ours	42.22	0.54	35.49	5	13
14	MBE	49.39	0.23	42.03	7	21
	Ours	50.86	0.63	42.45	6	15
16	MBE	56.45	0.23	48.05	8	24
	Ours	60.51	0.71	49.40	7	17
18	MBE	63.50	0.23	54.01	9	27
	Ours	69.15	0.80	56.36	8	19
20	MBE	70.56	0.23	60.00	10	30
	Ours	77.79	0.89	63.38	9	21
24	MBE	84.67	0.23	71.96	12	36
	Ours	95.08	1.06	77.23	11	25
32	MBE	112.90	0.23	95.89	16	48
	Ours	129.65	1.41	105.14	15	33

Multiplier Performance Comparison				
bit	Method	Area	Delay	Power
INT8	DW IP	291.6	1.87	211.4
	MBE	292.7	1.86	212.2
	Ours	290.4	1.99	210.3
	RME_Ours	264.4	1.63	188.9

Table 1: Area/ μm^2 , Delay/ ns and Power/ μW .

energy costs using PrimeTime PX based on VCD waveform files obtained from simulation with typical corner process.

4.2 Performance of the Encoder

In Table. 1, we ran performance tests on encoders for both 2-bit and multi-bit cases. In the comparison of resource consumption for 2-bit encoders, our method requires one less AND gate but one additional XNOR gate compared to MBE. This is because the

XOR logic is used to generate the sum for both 2 bits in Eq. 17. Although our individual encoder is at a disadvantage in terms of area, in the case of multi-bit encoding tests, our encoding representation requires one less encoder due to the fact that the lowest 2 bits do not need encoding. Therefore, our method only exhibits advantages in terms of area and power consumption when the encoding bit width is less than 14 bits. In terms of latency, due to the parallel computation nature of MBE encoding, the extended bit width has almost no impact on its latency. However, our encoding is based on carry-chain encoding, causing the latency to gradually increase with the width of the multiplicand. This is a drawback of our method, but it becomes an insignificant factor in the EN-TensorCore architecture, as the encoders will be placed outside the array and enter the array through registers. At this point, the true critical path lies within the adders and accumulators inside the PE. Lastly, in terms of the comparison of encoding bit width, our encoding representation is not sensitive to the data bit width, whereas MBE’s data bit width increases by a factor of 1.5. From the perspective of a single multiplier, this may not be an important factor. However, in the EN-TensorCore architecture, it becomes an obstacle that limits the performance improvement of the array. We also conducted performance tests on multipliers, using Synopsys DesignWare standard process library multiplier (DW IP) and Modified Booth Multiplier as benchmarks. In terms of INT8 performance, the area and power consumption are comparable to those of DW IP, with a slightly higher delay of 0.12ns. However, this is not the primary factor. We designed it specifically for the EN-TensorCore architecture. In the experiments after removing the encoder logic (RME_Ours), there are significant improvements in area, delay, and power consumption, making it a promising solution for achieving significant performance improvements in large-scale TCUs.

4.3 Performance of EN-TensorCore

We did performance tests on EN-TensorCore within the scope of mainstream AI accelerators, covering various tensor computation microarchitectures: 2D Matrix (Fig. 2(a)), 1D/2D Array (Fig. 2(b)), two types of Systolic Array (WS and OS) (Fig. 2(c)(d)), and 3D Cube (Fig. 2(e)). The array sizes will be tested at 16², 32², 64² (Cube: 4³, 8³, 16³) to evaluate the scalability, energy efficiency, and area efficiency of the EN-TensorCore architecture (Fig. 3(c)). The benchmark object for testing is the PE composed of Synopsys DesignWare standard

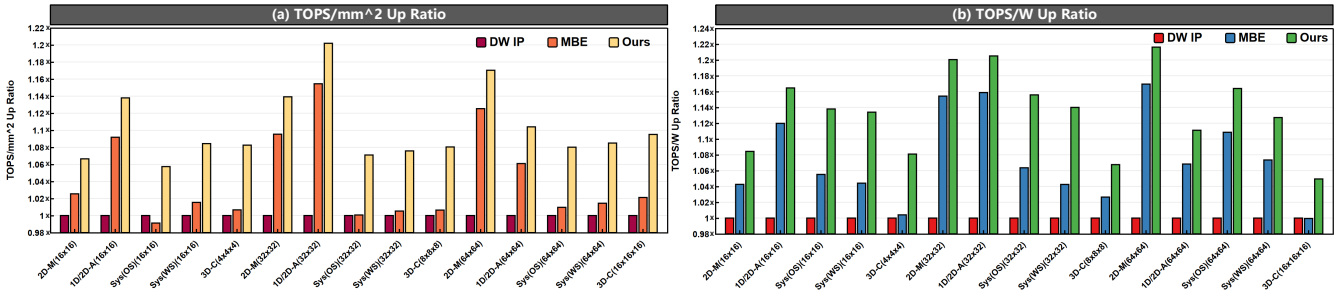


Figure 6: Up Ratio of Area Efficiency and Power Efficiency

process library multiplier. The EN-TensorCore architecture utilizes two encoders (MBE and Our Encoder) with register outputs, and all test on 500MHZ. The accuracy of multipliers in the PE is INT8 (Due to the prevalent use of INT8 in existing AI accelerators and edge devices, where the mantissa part of floating-point numbers often involves low-bit-width unsigned multiplication (BF16(UINT7), TF32(UINT10)), we adopt INT8 as the multiplication bit width for testing TCUs.), and the accumulator width is $16+\log_2 S$. S represents the array size.

In the area test (Fig. 5(a)(b)(c)), EN-TensorCore with MBE encoder demonstrates sensitivity to architectures. Even though the area of S^2 encoders is removed, the reduction in area is not significant in TCUs based on pipelined transfer, such as Systolic Array and 3D Cube. In some cases, there may even be an increase in area. This is due to the high data bit width of MBE encoding, which incurs the cost of S^2 4-bit registers for transferring this data in Systolic Array. However, in data broadcast-based 2D Matrix and 1D/2D Array, there is no such area overhead, and the removed logic can compensate for the impact of MBE's extra layout wire width. On the other hand, our approach further compresses the data line width in EN-TensorCore, enabling its relative advantages over MBE in TCUs based on pipelined transfer. Therefore, our encoding strategy can achieve significant area reduction in these architectures, making the array more compact and efficient. In the power test (Fig. 5(d)(e)(f)), both EN-TensorCore with MBE encoder and our encoder achieved significant reductions compared to the baseline. This is different from the area test. The reason is that the power consumption of an MBE 8-bit encoder is $24.07\mu W$, while the additional power consumption for transferring 4-bit registers is approximately $15.13\mu W$. The reduction in area also leads to shorter paths for data transfer between PEs, which helps further reduce power consumption. On the other hand, our encoder-based EN-TensorCore, benefiting from lower encoding bit width and area, can further reduce power from data transfer compared to MBE.

In the tests of energy efficiency and area efficiency (Fig. 6(a)(b)), we mainly compare the scalability of individual TCUs with different computational scales under EN-TensorCore. Due to the square relationship between the number of removed encoders and the array size, increasing the computational scale to a certain extent will result in higher performance. As shown in Fig. 6(a)(b), when the computational scale of our encoder-based EN-TensorCore expands from 256GOPS to 1TOPS and 4TOPS, the average area efficiency improves from 8.7% to 12.2% and 11.0%, and the energy efficiency improves from 13.0% to 17.5% and 15.5%, respectively. Among them,

the 1D/2D Array achieves a 20.2% increase in area efficiency and a 20.5% increase in energy efficiency compared to the baseline at 1TOPS. This is due to the specific characteristics of the multiplier-adder architecture itself (with no PEs, multipliers and multiplicands are not pipelined to the adder tree). In this case, the performance improvement of the EN-TensorCore architecture is the highest.

REFERENCES

- [1] S. Markidis, S. W. Der Chien, E. Laure, I. B. Peng, and J. S. Vetter, "Nvidia tensor core programmability, performance & precision," in *2018 IEEE international parallel and distributed processing symposium workshops (IPDPSW)*, pp. 522–531, IEEE, 2018.
- [2] S. Cass, "Taking ai to the edge: Google's tpu now comes in a maker-friendly package," *IEEE Spectrum*, vol. 56, no. 5, pp. 16–17, 2019.
- [3] Z. Jia, B. Tillman, M. Maggioni, and D. P. Scarpazza, "Dissecting the graphcore ipu architecture via microbenchmarking," *arXiv preprint arXiv:1912.03413*, 2019.
- [4] R. Prabhakar, S. Jairath, and J. L. Shin, "Sambanova sn10 rdu: A 7nm dataflow architecture to accelerate software 2.0," in *2022 IEEE International Solid-State Circuits Conference (ISSCC)*, vol. 65, pp. 350–352, IEEE, 2022.
- [5] H. Liao, J. Tu, J. Xia, H. Liu, X. Zhou, H. Yuan, and Y. Hu, "Ascend: a scalable and unified architecture for ubiquitous deep neural network computing: Industry track paper," in *2021 IEEE International Symposium on High-Performance Computer Architecture (HPCA)*, pp. 789–801, IEEE, 2021.
- [6] J. Li and Z. Jiang, "Performance analysis of cambricon ml100," in *Benchmarking, Measuring, and Optimizing: Second BenchCouncil International Symposium, Bench 2019, Denver, CO, USA, November 14–16, 2019, Revised Selected Papers 2*, pp. 57–66, Springer, 2020.
- [7] "Snapdragon 8 gen 3 mobile platform," 2023. <https://www.qualcomm.com/products/mobile/snapdragon/smartphones/snapdragon-8-series-mobile-platforms/snapdragon-8-gen-3-mobile-platform>.
- [8] "Mediatek dimensity 9300," 2023. <https://www.mediatek.com/products/smartphones-2/mediatek-dimensity-9300>.
- [9] "Apple a17," 2023. https://en.wikipedia.org/wiki/Apple_A17.
- [10] T. Chen, Z. Du, N. Sun, J. Wang, C. Wu, Y. Chen, and O. Temam, "Diannao: A small-footprint high-throughput accelerator for ubiquitous machine-learning," *ACM SIGARCH Computer Architecture News*, vol. 42, no. 1, pp. 269–284, 2014.
- [11] Y. Chen, T. Luo, S. Liu, S. Zhang, L. He, J. Wang, L. Li, T. Chen, Z. Xu, N. Sun, et al., "Dadiannao: A machine-learning supercomputer," in *2014 47th Annual IEEE/ACM International Symposium on Microarchitecture*, pp. 609–622, IEEE, 2014.
- [12] J. Wu, J. Zhou, Y. Gao, Y. Ding, N. Wong, and H. K.-H. So, "Msd: Mixing signed digit representations for hardware-efficient dnn acceleration on fpga with heterogeneous resources," in *2023 IEEE 31st Annual International Symposium on Field-Programmable Custom Computing Machines (FCCM)*, pp. 94–104, IEEE, 2023.
- [13] E. Talpes, D. D. Sarma, G. Venkataramanan, P. Bannon, B. McGee, B. Floering, A. Jalote, C. Hsiung, S. Arora, A. Gorti, et al., "Compute solution for tesla's full self-driving computer," *IEEE Micro*, vol. 40, no. 2, pp. 25–35, 2020.
- [14] "Nvidia a100 tensor core gpu," 2020. <https://www.nvidia.cn/data-center/a100/>.
- [15] A. A. Farooqui and V. G. Oklobdzija, "General data-path organization of a mac unit for vlsi implementation of dsp processors," in *1998 IEEE International Symposium on Circuits and Systems (ISCAS)*, vol. 2, pp. 260–263, IEEE, 1998.
- [16] J.-Y. Kang and J.-L. Gaudiot, "A fast and well-structured multiplier," in *Euromicro Symposium on Digital System Design, 2004. DSD 2004*, pp. 508–515, IEEE, 2004.
- [17] J. Kang, W. Lee, and T. Han, "A design of a multiplier module generator using 4-2 compressor," in *Proc. Korea Inst. of Telematics and Electronics (KITE) Fall Conf*, vol. 16, pp. 388–392, 1993.

- [18] W.-C. Yeh and C.-W. Jen, "High-speed booth encoded parallel multiplier design," *IEEE transactions on computers*, vol. 49, no. 7, pp. 692–701, 2000.
- [19] C. S. Wallace, "A suggestion for a fast multiplier," *IEEE Transactions on electronic Computers*, no. 1, pp. 14–17, 1964.
- [20] M. R. Santoro and M. A. Horowitz, "Spim: a pipelined 64* 64-bit iterative multiplier," *IEEE journal of solid-state circuits*, vol. 24, no. 2, pp. 487–493, 1989.
- [21] J. L. Hennessy and D. A. Patterson, *Computer architecture: a quantitative approach*. Elsevier, 2011.